HHS Public Access

Author manuscript

Bone. Author manuscript; available in PMC 2022 September 01.

Published in final edited form as:

Bone. 2021 September ; 150: 116002. doi:10.1016/j.bone.2021.116002.

Sexual differences in bone porosity, osteocyte density, and extracellular matrix organization due to osteoblastic-specific *Bmp2* deficiency in mice

Zacharie Toth, BS[#1,2], **Ashley Ward, BA**[#1,2], **Simon Y. Tang, PhD**[3], **Sarah McBride-Gagyi, PhD**[2]

[1]Authors Contributed Equally to this Work

[2]Department of Orthopaedic Surgery, Saint Louis University, St. Louis, MO

[3]Department of Orthopaedics, Washington University in St. Louis, St. Louis, MO

[#] These authors contributed equally to this work.

Abstract

Clinical studies have come to conflicting conclusions regarding BMP2 deficiency's link to regulating bone mass and increasing fracture risk. This may be due to the signaling protein having sex- or age-dependent effects. Previous pre-clinical studies have supported a role, but have not adequately determined the physical mechanism causing altered bulk material properties. This study investigated the physical effects of *Bmp2* ablation from osteogenic lineage cells (Osx-Cre;*Bmp2*$^{fl/fl}$) in 10- and 15-week-old male and female mice. Bones collected post-mortem were subjected to fracture toughness testing, reference point indentation testing, microCT, and histological analysis to determine the multi-scale relationships between mechanical/material behavior and collagen production, collagen organization, and bone architecture. BMP2-deficient bones were smaller, more brittle, and contained more lacunae-scale voids and cortical pores. The cellular density was significantly increased and there were material-level differences measured by reference point indentation, independently of collagen fiber alignment or organization. The disparities in bone size and in bone fracture toughness between genotypes were especially striking

Corresponding Author Contact Information: 1402 S. Grand Blvd, Schwitalla Hall M176, St. Louis, MO 63132, 314-977-8391, Sara.McBrideGagyi@health.slu.edu.

Individual Contributions:

Zacharie Toth: Methodology, Investigation, Formal Analysis, Writing - Review & Editing,**Ashley Ward:** Formal Analysis, Writing - Original Draft, **Simon Tang:** Methodology, Resources, Formal Analysis, Writing - Review & Editing, **Sarah McBride-Gagyi:**Conceptualization, Methodology, Investigation, Formal Analysis, Project Administration, Resources, Writing - Original Draft, Writing - Review & Editing

Disclosures:

Zacharie Toth: None

Ashley Ward: None

Simon Tang: Unpaid scientific advisor for Active Life Scientific; Secretary for the Orthopaedic Research Society's Spine Section

Sarah McBride-Gagyi: Volunteer for the Orthopaedic Research Society's International Section of Fracture Repair's Education Initiatives Committee

in males at 15-weeks-old. Together, this study suggests that there are sex- and age-dependent effects of BMP2 deficiency. The results from both sexes also warrant further investigation into BMP2 deficiency's role in osteoblasts' transition to osteocytes and overall bone porosity.

Keywords

Genetic Animal Models; BMP2; Bone Quality; Bone uCT; Histology

1. Introduction:

Bone morphogenic protein-2 (BMP2) is commonly used for promoting regeneration by inducing stem cell osteo- and chondro- genic differentiation *in vitro* and bone formation *in vivo* [1]. Thus, the condition of *exogenous* BMP2 has been extensively studied. However, investigations into BMP2 *deficiency* are lacking. Given the protein's prominent role in stimulating bone formation and promoting osteoblast function, it would be logical to assert that the loss of BMP2 would affect bone mass and fracture risk. Yet there is no consensus on the effects of BMP2 on bone mass and fracture incidence in clinical studies [2–10]. Some studies have found a significant relationship between BMP2 and decreased bone mineral density (BMD) or increased fracture risk[2,3,6,8,11], while others report unremarkable or weak relationships[4,5,9,10]. One possible reason for these conflicting conclusions could be that BMP2 acts in a sex-dependent manner. For example, Choi *et al.* found the same *Bmp2* polymorphism caused an increase in BMD in young males while it caused a decrease in BMD in their female counterparts[8]. Xiong *et al.* found *Bmp2* polymorphisms to have a similar negative correlation with radius BMD in both sexes, but spine and hip BMD were only significantly correlated for females[6]. These differences may also be age-dependent. Some of these studies focused only on younger individuals (<50)[8,9], some only older[3,5,10], and some a mix[2,4,6].

Pre-clinical studies have demonstrated a role for BMP2 in regulating bone quantity and fracture resistance[12–17]. Depletion of BMP2 in bone lineage cells results in a spectrum of bone quality deficiencies. The phenotype varies with the stage of lineage commitment, with the most severe manifestation occurring during early cell fate. Ablation of BMP2 from osteochondro-progenitors using the limb-specific Prx1-Cre results in severe skeletal defects. While newborns' skeletons seem relatively normal, as early as 1 week of age differences like delays in secondary ossification centers and joint malformations become apparent.[12,13,18] By two weeks femora are significantly shorter and more narrow.[18] BMP2-deficient adult mice remain smaller than their control littermates and appear to have compromised bone quality in addition to quantity. Mice with this transgenic manipulation exhibit spontaneous fractures that increase with age, and the fractures fail to mount the early stages of healing [13,17,18]. Three-point bending tests of whole bones demonstrated that BMP2 deficient bones are stronger per unit area but significantly more brittle[17]. Ablating BMP2 from osteoprogenitors using OSX-Cre[16,19] or 3.6Col1a1-Cre[15] also results in reduced stature and per unit area stronger but more brittle bones. However, these BMP2-deficient bones do not spontaneously fracture. When the ablation was delayed until weaning, bones from 12 week-old BMP2-deficient mice were more similar in size to their control littermates but still

showed altered material properties[19]. It remains unclear whether the apparent mechanical deficits observed are related to the molecular-level material properties of BMP2 deficient bone or cell- and tissue-scale architectural features than can also result in brittle behavior.

The deterioration in bone mechanical properties can span multiple length scales from whole bone geometry down to the material level behavior. Cortical geometry is associated with the stiffness and absolute strength of bone, and increased moments of inertia leading to stiffer bones that are capable of withstanding increased loads with less deformation[20]. Intracortical features such as cortical porosity increase with age and reduces bone strength per unit volume[21]. The structural complexity of intracortical canal networks, which house bone vasculature and remodeling units, has been shown to increase porosity and reduce fracture toughness of long bones[22]. Bone's *material* properties at the sub-cellular level primarily depend on the organization and interactions of its two main compositional components, hydroxyapatite and type I collagen. It is generally thought that the mineral hydroxyapatite determines tissue level stiffness while type I collagen is governs post-yield behavior following plastic deformation and overall toughness[20].

Prior work suggests that deficient BMP2 production in osteo-chondro-lineage cells affect the bone strength and quality on multiple length scales. While bones with loss of osteoblast-derived BMP2 did not exhibit differences in organic matrix and mineral composition, [16] these animals exhibit reduced ductility at the whole-bone level, indicating a potential defect in organization of the extracellular matrix rather than changes in cellular production. [16] The increased brittleness could also be due to increased cortical porosity. Prior BMP2 ablation studies showed incongruence between the whole body mineral density (measured by DeXA)[13,16,23] and tissue mineral density (measured by microCT)[16], but other cortical features such as porosity were not examined.

In this study, we sought to characterize the effects of BMP2 deficiency on bone mass accrual, to better determine the physical mechanism of brittleness in BMP2 deficient bones, and to investigate if the effects of BMP2 deficiency were sex and/or age dependent. BMP2 deletion was targeted to the osteoblast lineage using a tetracycline-controlled Osx-Cre promoter with ablation occurring during animal weaning. Bone fracture mechanics, reference point indentation, and structure at multiple length scales were assessed cross-sectionally at 10-weeks and 15-weeks of age. We hypothesized that BMP2 deficient bones would be smaller and mechanically inferior due to either increased porosity, dysregulation of collagen production/organization, or a combination of these. Further, we hypothesized that these differences would be sexually dependent and worsen with aging.

2. Materials and Methods:

2.1. Animals:

All studies were performed in strict adherence to the Guide for the Care and Use of Laboratory Animals of the National Institutes of Health. The protocol was approved by the IACUC of Saint Louis University (Protocol Number: 2382). Mice were group housed under standard conditions with 12 hour light/dark cycles with standard chow and water *ad libitum.*

Euthanasia was carried out in compliance with American Veterinary Medicine Association Guidelines.

To create experimental mice, female mice with the *Bmp2* floxed gene (*BMP2*$^{fl/fl}$[16,19] were crossed with male mice possessing the same *Bmp2* floxed gene and a tetracycline-controlled Osterix-Cre promoter ((B6.Cg-Tg(Sp7-tTA,tetOff-EGFP/Cre)1Amc/J, Jackson Laboratories, Bar Harbor, ME). Mice that were homozygous for the *Bmp2* floxed gene but lacked Cre were used as controls (control, *Bmp2*$^{fl/fl}$). Littermate mice that possessed the floxed *Bmp2* alleles and at least one Osterix-promoted Cre served as the experimental mice (cKO, *Osx-Cre;Bmp2*$^{fl/fl}$). In the absence of tetracycline administration, BMP2 is removed from early-stage osteoblasts in cKO animals, which persists throughout the maturation of the osteoblasts and osteocytes. For this study, doxycycline treated water was administered to all breeding cages so both control and cKO mice received doxycycline. Thus, ablation was repressed through gestation and early post-natal stages until weaning (P21) at which time both control and cKO mice were switched to doxycycline-free water (and therefore induction of Cre recombination in Osx+ cells). Previous qPCR has shown this recombination to have approximately 60% efficiency in uninjured animals whether the cre-recombination is repressed with doxycycline or not.[19] Animal genotype was determined by PCR of DNA collected from tail snips taken at P7 to P10 using the following primers (floxed *Bmp2* allele F: 5’ - GTG TGG TCC ACC GCA TCA C - 3’, R: 5’ - GGC AGA CAT TGT ATC TCT AGG - 3’, *Cre* F: 5’-GCC TGC ATT ACC GGT CGA TGC A-3’, R: 5’-GTG GCA GAT GGC GCG GCA ACA-3’). We assessed both control and cKO mice at 10 and 15 weeks of age in females and males after euthanasia (7 and 12 weeks of cKO, respectively). These ages were chosen to roughly align with our previous work in 12 week-old mice and determine if differences attributable to BMP2 modulation were static or dynamic. Originally, 10 animals were produced for each group. However, some samples were lost during testing or processing, so the final group numbers for each outcome may differ. Test administrators were blinded to genotype to the extent possible given obvious physical differences. Right femora were harvested for fracture toughness mechanical testing, right humeri were harvested for reference point indentation of the mid-diaphysis, and left femora were harvested for cortical and cancellous bone measures (microCT and histology).

2.2. Fracture Toughness Mechanical Testing:

The right femora (n=7-10/group) were used for notched three-point bend testing[24]. Femora were cleaned of surrounding soft tissue and frozen in PBS-soaked gauze at −20°C. Twenty-four hours prior to three-point bend testing, bones were warmed to 37°C and manually notched at the midpoint on the posterior face using a steel-backed regular duty single edge razor blade. Notches were subsequently sharpened using the same blade irrigated with a 1 μm diamond suspension (MetaDi, Buehler, Lake Bluff, IL). Bones were stored in 1X PBS at 4°C overnight, warmed to 37°C for 1 hour, and subjected to three-point bending using a Criterion 42 Material Testing Workstation (MTS Systems Corporation, Eden Prairie, MN) with a support span of 4.51 mm. Bending was performed at a displacement rate of 0.001 mm/s until failure while recording force.

Samples were then scanned by microCT (uCT35, ScanCo Medical, Wayne, PA, X-ray potential 45 kVp, X-Ray intensity 88 μA, isotropic voxel size 6 μm, Integration Time 300 ms). Using the ScanCo software, each bone was contoured separately and then segmented using a threshold of 250 permilles (557.3 mgHA/ccm) with gauss sigma 0.8 and gauss support 1.0. The resulting 3D reconstructions were used to determine the half notch angle (ImageJ, NIH, Bethesda, MD)[25]. Fracture toughness, K_c, was calculated using the unstable cracking method for the propagation of a circumferential through-wall flaw in cylinders.

2.3 Reference Point Indentation:

To assess local material properties independent of whole bone geometry, reference point indention was performed. Right humeri (n=5-10/group) were cleaned of surrounding soft tissue and stored in PBS-soaked gauze at −20°C until the time of testing. Samples were warmed to 37°C, mounted to an acrylic test block with an epoxy resin, and indented at a frequency of 2 Hz under force control (2N) using a microindenter with a 90° cono-spherical indentation tip with a rounded 5 μm radius (BioDent, Active Life Scientific, Santa Barbara, CA). A polymethylmethacrylate block was used for calibration measurements before and after measurements for each sample to assure measurements did not drift. Three regions on the periosteal surface centered around the mid-diaphysis were indented per sample, spaced approximately 1 mm apart. A new tip was used for every five bone samples. The force-deformation data was collected during loading and unloading. The following parameters were calculated using a custom Matlab code: total indentation distance (TID), indentation distance increase (IDI), average energy dissipated, average loading slope, and average unloading slope.

2.4 MicroCT:

MicroCT was performed to determine cortical and cancellous bone measures. Left femora from control and cKO mice (n=8-10/group) were fixed approximately 48 hours in 10% neutral buffered formalin and then scanned by cone beam microCT twice (μCT 35, ScanCo Medical, Wayne, PA). First, each sample underwent a medium resolution (12 μm) scan of the whole bone (X-Ray potential 70 kVp, X-Ray intensity 114 μA, isotropic voxel size 12 μm, Integration Time 300 ms, Frame Averaging 1, 500 projections). This scan was used to determine overall femur length and medium resolution cortical measures using the built-in manufacturer's programs (gauss sigma: 0.8, gauss support: 1, threshold: 250 permilles). The following cortical bone outcomes were determined for a region starting at the femoral midpoint and extending 360 μm distally (30 slices) that included the marrow space: total cross-sectional area (Ct.Tt.Ar), cortical bone area (Ct.Ba.Ar), cortical bone fraction (Ct.Ba.Ar/Ct.Tt.Ar), tissue mineral density (TMD), cortical thickness (Ct.Th), maximal moment of inertia (I_{max}), and minimal moment of inertia (I_{min}). Next, a high-resolution scan (3.5 μm) was taken at the femur mid-point (X-ray potential 45 kVp, X-Ray intensity 88 μA, isotropic voxel size 3.5 μm, Integration Time 300 ms, Frame Averaging 2, 1000 projections). This scan was similarly analyzed using built-in manufacture's programs. The volume of interest for these scans started at the femur midpoint and extended distally for 105 μm (30 slices) while excluding the marrow. It was used to determine cortical porosity or space

volume fraction (Space/TV = 1 – bone volume fraction), average pore diameter, and volumetric tissue mineral density (vTMD).

2.5 Histology:

Histological analyses were performed to assess collagen fiber packing and alignment, remnant woven bone fraction, porosity, and cellularity. Following microCT scanning, left femora were decalcified with formic acid, rinsed in PBS, cut at the femoral midpoint, dehydrated in ethanol, and embedded in paraffin. Paraffin sections were obtained in the coronal plane at 5 μm thickness and subsequently stained. One section per animal was stained with Weigert's hematoxylin, picrosirius red, and Alcian blue. Picrosirius red enhances the birefringence of collagen fibers, allowing for the assessment of relative collagen fibril orientation and indirectly measuring fibril thickness. Sections were imaged under polarized and compensated light in 15° increments from 0° to 180°. These images were used to assess collagen alignment and hue, which is an indirect measurement of fiber size or packing, for a small region of interest containing predominately lamellar bone in the posterio-lateral quadrant. The resultant vector, a dimensionless value ranging from zero to one in length, defines the circular spread of a data set; the closer the length of the resultant vector is to one, the more concentrated the data sample is around the mean direction (i.e., if all collagen fibers are oriented in the same direction, the resultant vector will have length close to one).[26,27] An additional polarized image of the whole cross section taken at a single phase was captured to determine the relative amount of remnant woven bone present (remnant woven bone fraction of total bone area).[28] Finally, the same section was then imaged under green fluorescent light (20x magnification) to accentuate void spaces (lacunar, vascular, etc.) within the cortical cross section to determine relative areal porosity (pore area per total bone area). Areas of calcified cartilage, which are irregularly shaped and appear blue in the brightfield images and dark on the fluorescent images, were excluded from analysis. Schneider et al reported an average lacuna volume of approximately 200 μm^3 in the C57BL/6J strain.[22] Based on back-calculations that assumed a circular cross-section of an elliptical solid, a 50 μm^2 threshold was implemented; voids less than this threshold were counted as lacunae while those greater than this threshold were counted as canals. Serial sections were stained with DAPI and imaged under fluorescent UV light to measure areal cellularity (number of cell nuclei normalized to total bone area) of the entire cross-section. Collagen alignment (n=5-10/group), areal porosity (n=8-10/group), and cellularity (n=6-10/group) measures were obtained through custom MatLab codes while remnant woven bone fraction (n=6-10/group) was performed via ImageJ.

2.6 Statistics:

Data is presented as box plot with individual data points overlaid. First normality for each outcome was assessed using Wilks-Shapiro testing (RStudio Version 1.2.5033, RStudio Inc, Boston, MA). If data met this assumption as is or with a natural log transformation, it was analyzed using a multivariate ANOVA (factors: genotype, age, and sex). If data could not be analyzed in this manner, it was split to attempt to analyze females and males separately. Again, the segregated data (as is or with a natural log transformation) was first tested for normality using Wilks-Shapiro and, if it met this assumption, was analyzed using multivariate ANOVA (factors: genotype, age). For both methods, if any of the factors or

interactions were significant, post-hoc pair-wise analysis was done using Tukey. For data that could not be analyzed using any of the previous methods, pair-wise comparisons were done between genotypes at each age/sex using Mann-Whitney testing. The corresponding statistical method used for each outcome and the respective p-values for each factor/interaction is presented in Tables 1 and S1. Graphs present the p-values for each significantly different pair-wise comparison (Tukey or Mann-Whitney).

3. Results:

3.1 Fracture Toughness Testing:

Right femora notched on the posterior surface of the mid-diaphysis were subjected to three-point bending to elucidate differences in fracture resistance between cKO bones and littermate controls (Figure 1A). Male cKO femora failed at significantly lower loads compared to littermate controls at both 10 and 15 weeks while control males failed at significantly higher loads than control females at both ages (Figure 1B). No differences in half-notch angles were observed between groups, indicating similar stable crack extensions in all groups (Figure 1C). While there was a significant trend for cKO bones to have reduced fracture toughness (K_C), the differential in males increased from 10 to 15 weeks to reach pair-wise significance. In contrast, the difference in females remained relatively constant between the two ages (Figure 1D). Taken together this confirms the previous work indicating a deficiency in post-yield mechanical behavior at the tissue level, and advances that work by showing it is more pronounced in male mice with advancement in skeletal maturity.

3.2 Reference Point Indentation:

To determine if the mechanical deficiencies were also a product of material defects rather than higher length-scale architectural differences, reference point indentation was performed. Overall the differences between groups was mild. In general, cKO bones had a slightly higher total indentation distance, but there were no pair-wise differences between individual groups (Figure 2A). This may be due the study not being sufficiently powered for Tukey adjustments for all the post-hoc comparisons. Indentation distance increase was significantly higher in cKO bones for the 10-week-old females and 15-week-old males (Figure 2B). Average loading slope was significantly lower for 15-week-old cKO males (Figure 2D). There were no differences in average energy dissipated or average unloading slope (Figures 2C and 2E).

3.3 MicroCT:

MicroCT analysis was performed on left femora to determine cortical bone measures (12 μm and 3.5 μm resolution, Figures 3 and 4, respectively). In both sexes, cKO bones were shorter and smaller than control bones as shown by the decreased femur length and total cortical area (Figures 3B and 3C). Bone area, however, was not as greatly affected by genotype (Figure 3D). It was still significantly smaller in cKO bones especially at 15 weeks old, but the cortices were significantly thicker (Figure 3G) resulting in significantly higher bone volume fractions (Ba.Ar/Tt.Ar, Figure 3E) at both ages in both sexes. Despite these increases in cortical thickness and Ba.Ar/Tt.Ar, cKO bones had significantly reduced moments of inertia (i.e. Imax and Imin, Figures 3H and 3I). As demonstrated in Figure 3A,

the bone material itself was distributed closer to the centroid in cKO bones. Interestingly, several structural measurements (i.e. femur length, total area, and moments of inertia) increased between the two ages for control bones but not for cKO bones suggesting that cKO mice have delayed growth during this late adolescent time period. This was especially true for the males. Similar results were observed in the trabecular compartment (Figure S2). Of note, in many instances the differences between genotypes remained even when normalized for animal body weight (Figure S4).

Scanning at high resolution (3.5 μm) revealed 20 to 40 μm diameter canals radiating into the endosteal surface of cKO bones (Figure 4A, also visible in medium resolution scan Figure 3A). Quantification demonstrated a significantly higher overall porosity (Space/TV, Figure 4B) and average pore diameter (Figure 4C) in cKO bones.

When tissue mineral density was assessed at the 12 μm resolution (Figure 3F), it was significantly lower for cKO bones and higher with aging in general; although in pair-wise comparisons it was only significant for the 10-week-old female controls and cKOs. When assessed at 3.5 μm resolution (Figure 4D), the pair-wise comparisons between all genotype and age groups were significant. This suggests that the small pores contributed to partial volume affects at the 12 μm resolution causing increased variability. This data also suggests that there is a mineralization issue in the cKO bones of both sexes.

3.4 Histology:

To assess whether or not differences in mechanical strength were attributable to just the porosity differences or whether there was also an effect on collagen fibril organization or other cellular behavior, histology was used (Figures 5A and 5B). No differences in relative collagen orientation were found between groups (Figure 5C). No differences in fibril diameter/packing were observed between cKO bones and littermate controls. There were differences attributable to aging (Figure 5D) although the functional consequence remains to be investigated. Together this indicates collagen fibers in cKO bones were being organized properly at the microscale. At the tissue level, the remnant woven bone fraction was statistically higher in cKO bones and males (Figure 5E). However, here the differential in males decreased with aging while it stayed relatively the same for females.

Since only mild defects in collagen regulation were observed, we sought to corroborate three-dimensional microCT porosity data with an areal porosity measure of picrosirius red stained paraffin sections (Figure 6A). Because of the non-normal distribution of areal porosity fraction data, comparisons as a whole were not possible. There appears to be trends for cKO bones to be more porous, but it was only significant for 15-week-old females (Figure 6B). Furthermore, we asked whether these differences in porosity were attributable to increases in lacunar scale voids or vascular canal scale voids. When normalized for cortical area, cKO bones contained significantly more lacunae-scale voids than controls (Figure 6C). The pair-wise comparisons were significant for all ages/sexes. Canal-sized void density was generally higher in cKO and males (Figure 6D). However, the only pair-wise difference was between control females and males at 15-weeks-old. Serial paraffin sections stained with DAPI substantiated areal porosity measures with cKO bones having significantly more cells per unit area (Figure 7). Similar to the lacunae-sized voids, the pair-

wise comparisons were significant for 3 of the 4 genotype comparisons. The differential decreased for males from 10 to 15 weeks old.

4. Discussion:

Previous human studies have come to conflicting conclusions as to whether the signaling protein BMP2 plays an important role in governing bone mass and fracture resistance. Some results suggest that the discrepancy might be related to sex- or age-related effects. Pre-clinical work has generally supported a role for BMP2 in bone mass and quality. However, the possible mechanism resulting in mechanically deficient bones was unclear, and its possible effects had not been adequately compared between sexes. This study's aim was to build-upon our previous observations about decreased mechanical properties in animals lacking BMP2 in osteoblast and osteocytes by clarifying both the structural and material differences on multiple length scales. We also sought to determine if there were sex-related or aging effects during late adolescence. In accordance with our hypothesis, BMP2 knockout resulted in an increase in cortical porosity, with significantly more lacunae-scale voids and average pore size compared to control animals. However, contrary to our hypothesis, differences in collagen fiber organization or size/packing at the sub-cellular level did not fully explain the mechanical differences observed in the BMP2 cKO animals. Further, our data supports a sex-dependent role of BMP2 in bone growth. However, it is unclear if this is a true sexual dimorphism rather than an equal effect on both sexes that negates the sexual dimorphism observed during normal growth. The expected age-related divergences between sexes - especially overall bone growth - did not always occur in knockout animals. Thus, cKO males' size increasingly diverged from controls as they aged.

Structurally, femora of cKO mice were shorter, smaller, and have thicker cortices at both ages when compared to littermate controls. In addition, cKO mice showed significantly impeded growth, with little to no change in femoral length, total cross sectional area, bone area, or moments of inertia between 10 and 15 weeks. This was especially evident in males, which may be due to this strain's differential growth rates between the two ages investigated. Body weights typically increase by −12% for females and −17% for males from 10 to 15 weeks[29]. Our controls followed this pattern, but cKO mice remained at relatively the same weight (Figure S4). However, even when normalized for body weight, cKO bones were consistently different in overall size (Figure S4). These results are consistent with our previous work which showed that cKO mice are smaller, possessing shorter tibia throughout life[16]. However, in the previous work, the lower total and bone area in males was significantly different in the younger of the two time points, 12-weeks-old, but only a non-significant trend in the 24-week cohort. It was the opposite in this current project with outcomes being more differential at the older time point, 15-weeks-old. This could be evidence of site specific differences or could indicate that eventually male cKO mice close the gap to normal controls as growth velocity slows in control animals. In contrast, previous work showed the smaller tibia phenotype (length, total volume, and bone volume) was evident in cKO females at 24-weeks-old. Taken together with the current study's evident robust effects on males from 10 to 15 weeks, this may point to a sexual difference with some contextual dependency on age. Contrary to our previous work with this mouse line, cortical TMD as assessed by microCT was decreased in cKOs. This became more evident in the

higher resolution scans where void spaces could be better resolved and did not contribute to partial volume effects when calculating TMD. Again, this could be a site-specific difference between tibia and femora. This also agrees well with the findings of Yang *et al.* which used a slightly different model to remove BMP2 from osteogenic lineage cells. [15] Overall, this whole bone structural phenotype is similar, but less severe, than when BMP2 is ablated from all osteo- and chondro-progenitor cells using Prx1-Cre.[13,17,18]

In order to probe the determinant of whole bone mechanical behavior, fracture toughness and reference point indentation were undertaken. As expected given the size discrepancies and paralleling previous findings, notched cKO femora failed at significantly lower loads. Fracture toughness of cKO animals was lower compared to littermate controls, with differences more striking in males with increased age. This confirms that at the organ or tissue-level, the cKO bones are more brittle and supports a sex-dependent effect on the apparent strength in addition to size. cKO bones may perform similarly under physiological loading, but will fail quickly once yield stress/strain is reached. Reference point indentation showed some mild differences with total indentation distance being increased in cKO bones. Average loading slope was lower in male cKO bones at 15 weeks of age.

Further analysis of the bone structure and collagen organization suggest that the collagen organization is largely unaffected at the sub-cellular level, and that higher length-scale issues are a major contributor to the brittleness. MicroCT and histology showed a substantial increase in porosity in all cKO mice at all time points. High resolution microCT revealed significantly higher space fraction per unit volume in cKO bones. Canal-like voids emanating from the endosteal surface of the femoral midshaft of cKO bones were consistently observed, which skewed the average pore diameter to be higher in cKO bones. Histology, which has even higher resolution and is better able to resolve lacunae-scale voids, showed increased lacunae-scale pores in cKO bones similar to *Bmp2* ablation with Prx1-Cre[18]. The increase in canal-sized pores was not as distinct as we would have expected from the microCT reconstructions. Also, there were no consistent differences in overall space fraction via histology. Both canal-sized voids and their contributions to overall space fraction could be inaccurately captured by histology due to sectioning bias. This would also explain the increased variation in these outcomes relative to lacunae-sized void density. In any material, an increase in porosity decreases fracture resistance, as each void not only reduces cross-sectional area, thus raising bulk stress, but also creates local stress concentrations causing failure at reduced overall load.

Decreased lamellar organization can have similar consequences to increased porosity. While there were differences in the relative amount of remnant woven bone, especially in 10 week old males, our previous work examining its contribution to strength in normal mice bones indicated only a weak relationship to one measurement, post-maximal energy to fracture. [28] Further, the relative amount of remnant woven bone in the current cKO bones was within range of our previous work with normal 13 week old mice (20 to 30%). Also, the difference in remnant bone fraction between controls and cKO bones decreases in males from 10 to 15 weeks while the difference in fracture resistance increased. It is thus unlikely that the increases in remnant woven bone fraction are greatly contributing to the brittle phenotype. When lamellar collagen fibrils were assessed, no differences in organization or

fibril diameter/packing (i.e. hue) were found between genotypes. However, picrosirius red staining and polarized light imaging is not the most sensitive test of collagen fibril defects. It is entirely possible that there are molecular-level effects like changes in post-translational modifications or collagen crosslinking that contribute to fracture behavior. There is evidence that BMP2 upregulates expression of genes for enzymes needed to create and process pro-collagen molecules into final tropocollagen molecules. [30,31] If creation and conversion is not correctly executed, tropocollagen molecules cannot correctly self-assemble into fibrils resulting in diminished bone strength. If this is the case, this may explain the decreased tissue mineral densities and differential reference point indentation results.

Our findings here contrast with somewhat with previous works. Yang *et al.* concluded from *in vivo* and *in vitro* studies that collagen production and mineralization was impaired causing the brittleness in their BMP2 knockout that utilized the 3.6Col1a1-Cre[15]. Our current study also demonstrated some issues with bone tissue mineralization but we doubt the differences are great enough to account for the large differences in brittleness observed in both studies. The collagen production conclusions in Yang *et al.* were mostly based on gene expression data of collagen rather than assaying the final protein product for protein structure defects. Higher length-scale architecture was not assessed nor was final collagen tropocollagen structure or crosslinking. Our cell nuclei density outcomes support their conclusions that something is impaired with osteogenic lineage progression and cell behavior; although, we did not determine if the increased cell nuclei density were specifically attributed to osteocytes. This is an assumption we are making based on the accompanying increased density of lacunae-sized voids. Assuming these are increased osteocytes, this is evidence that deficient BMP2 in osteogenic lineage cells is causing an increase in the number of osteoblasts transitioning to osteocytes. A similar effect was observed in BMP2 ablation with Prx1-Cre[18] and when osteoblast apoptosis was prevented. [32] Dysapoptosis lead to increased osteocytes and increased cortical porosity that worsened with aging. Coupled with the decreased overall size this suggests that BMP2-deficient osteoblasts may be ceasing collagen production activities too quickly and prematurely differentiating into osteocytes. So it is possible that that collagen *production rate* was affected in Yang *et al. 's* model which would agree with their gene expression findings. Also, our conclusions contrast with previous work where SMAD4, an important intracellular protein in the BMP2 signaling pathway, was deleted in osteo-lineage cells and lead to defects in collagen production as shown by similar methods used here (i.e. polarized light hue)[33]. However, these mice had a much more severe phenotype. It was similar to the Prx1-Cre knockout of BMP2 in that the bones were much more slender and prone to spontaneous fracture. This could simply reflect a difference in model. Signaling via this pathway, which is utilized by proteins other than BMP2, was still operational in our model but likely not as active due to the lower abundance of extracellular BMP2.

Our study does have some notable limitations and possible confounding variables that should be considered . First, a Cre-only control was not included. There is significant evidence that the OSX-Cre alone can have profound skeletal effects. Most notably OSX-Cre expression alone can cause skull hypomineralization[34,35], spontaneous intramembranous bone fractures[35], and reduced body size.[34–36] However, these effects are not present at birth[34,35], appear to peak in the first few weeks of life[34,36], and are not present at all by

12 weeks of age[36]. There is also ample evidence that OSX-Cre does not impact trabecular bone[34], which was impacted similarly to the cortical compartment in this study (Figure S2). Further, these skeletal defects are completely rescued with doxycycline administration in the early pre-natal period (to P21)[34]. Thus, since the OSX-Cre cKO mice in this study were examined at older ages, given doxycycline during the critical post-natal period when most differences have been noted, showed parallel size discrepancies in the trabecular compartment, and had a similar phenotype to BMP2 cKOs using different osteoblast-targeting Cre (3.6Col1a1-Cre[15]), it is relatively safe to conclude the observed differences of this study between genotypes is attributable to the BMP2 knockout not an off-target effect of the OSX-Cre alone. Second, while we attempted to do a very thorough investigation of the structural aspects of the bones at our disposal, we were not able to do higher resolution assays like atomic force microscopy or electron microscopy to better examine collagen organization as has been done with collagen processing disorders like osteogenesis imperfecta[37]. Nor was collagen crosslinking examined. So there could be differences attributable to molecular-scale characteristics that should be investigated. Along those lines, beyond verifying that *Bmp2* mRNA levels were reduced in cKO bones, no other attempts were made to quantify BMP2 content or demonstrate a reduction in BMP2-related signaling. When designing this study, BMP2 content or biological mechanisms were not the focus – identifying the physical elements affecting bone quantity and quality was our main objective. Thus, delving into this limitation was deemed beyond the project's scope and will be the focus of future work; but, in theory, there would be normal levels of matrix-bound BMP2 throughout control bone and in the central elements of the cKO bones laid down prior to removal of doxycycline and recombination (i.e. remnant woven bone band).[28] Also, given that there is a delay between when an osteoblast lineage cell starts producing the (*Osx*-controlled cre and actual recombination thus protein production cessation, there may likely be some or even normal levels of matrix-bound BMP2 throughout the newer cKO bone. An interesting future direction would be to quantify the relative amount of each bone's matrix-bound BMP2 as well as the timing/efficiency of ablation and then determine if that correlates with the differences observed here between sexes. To our knowledge no one has investigated whether sex- or age-dependent differences in *Osx*-Cre recombination timing or efficiency exist but there does not appear to be ample anecdotal evidence. Regardless, while BMP2 is a soluble signaling protein that can be matrix-bound, it does not appear to have structural roles. Thus it is unlikely that BMP2's presence (or absence) would have any *direct* effects on material behavior like differences in the quantity or quality of collagen type 1. Furthermore, BMP2 is not typically produced by more mature osteocytes in the central cortex [18]. Current evidence suggests that by 2 weeks of age only about half of cortical osteocytes, those closer to the expanding periosteal surface, express BMP2. As the animal ages, BMP2 expression becomes increasingly restricted to the periosteal surface and periosteum. An exception is during fracture repair, where osteocytes across the entire cortex, but within a limited distance of the fracture surface, revive BMP2 expression. ID1 expression, an indicator of BMP2 signaling, follows this expression pattern during growth. Together this suggests that osteoblast-and osteocyte-secreted BMP2 is highly autocrine and active mostly at the time of creation; that neither matrix-bound BMP2 nor BMP2 released by normal remodeling events appreciably affects cell behavior. For this study that would mean that differences in matrix-bound BMP2 content would have little to no effect on the

outcomes. Finally , the two ages selected for this study are both still relatively young roughly representing 18 and 22 year old humans, respectively, rather than 25 and 65.[38] However, it is striking that differences still exist even at these young age groups. It may also indicate that BMP2 deficiency detrimentally affects attainment of peak bone mass as a young adult which, as established, can have consequences in the later decades of life.

In conclusion, the knockout of BMP2 using an osterix-promoted Cre resulted in limbs that were both shorter and mechanically inferior. Our findings indicate that this knockout does not dramatically affect collagen fibril organization or size. However we cannot rule out molecular-scale defects in the bone matrix attributable to collagen creation, processing, or crosslinking that would not be obvious with the methods used here (i.e. polarized light imaging). The bones of cKO mice were consistently found to be substantially more porous than those of littermate controls. This indicates that increased porosity possibly as a product of abnormal lineage maturation of osteoblasts to osteocytes is major contributor to the structural and material differences of BMP2-deficient bones. Further, our findings support a sexually dependent role of BMP2 which deserves further investigation. All cKO bones had lower fracture toughness than their respective controls. However, the differential increases in males from 10 to 15 weeks while it stays relatively stable in females between the two ages. Porosity alone does not explain this result since all porosity measures either remained constant across sex/ages for both genotypes or changed similarly in males and females from 10 to 15 weeks. Bone size followed the same sexually dependent pattern as fracture toughness but fracture toughness outcomes normalize for size so we do not feel they are directly related. Furthermore, there could be differing amounts of matrix bound BMP2 in our groups which could affect the outcomes. To our knowledge, there have been few pre-clinical or mechanistic studies to compare BMP2 deficiency between sexes in any organ system and none in bone. A couple studies have indicated exogenous BMP2 differentially affects osteogenic differentiation of stem cells from males and females.[39,40] Using this mouse model, additional investigation into targeted osteoblast or osteoclast pharmacological therapies to counteract the mechanisms causing bone brittleness such as age-related porosity may be warranted.

Supplementary Material

Refer to Web version on PubMed Central for supplementary material.

Acknowledgements:

We would like to thank Dan Lieb for technical assistance with the reference point indentation testing and Megan Killian and Matt Allen for critical manuscript feedback and project interpretation thoughts. No direct grant funding was received for these studies, but it was supported indirectly by the by the Washington University Musculoskeletal Research Center (MRC) (NIH P30 AR074992).

References:

[1]. Rosen V, BMP2 signaling in bone development and repair., Cytokine Growth Factor Rev. 20 475–80. 10.1016/j.cytogfr.2009.10.018.

[2]. Styrkarsdottir U, Cazier J-B, Kong A, Rolfsson O, Larsen H, Bjarnadottir E, Johannsdottir VD, Sigurdardottir MS, Bagger Y, Christiansen C, Reynisdottir I, Grant SFA, Jonasson K, Frigge ML, Gulcher JR, Sigurdsson G, Stefansson K, Linkage of osteoporosis to chromosome 20p12 and

association to BMP2., PLoS Biol. 1 (2003) E69. 10.1371/journal.pbio.0000069. [PubMed: 14691541]

[3]. Tranah GJ, Taylor BC, Lui L-Y, Zmuda JM, Cauley JA, Ensrud KE, Hillier TA, Hochberg MC, Li J, Rhees BK, Erlich HA, Sternlicht MD, Peltz G, Cummings SR, Genetic variation in candidate osteoporosis genes, bone mineral density, and fracture risk: the study of osteoporotic fractures., Calcif. Tissue Int. 83 (2008) 155–66. 10.1007/s00223-008-9165-y. [PubMed: 18787887]

[4]. McGuigan FE, Larzenius E, Callreus M, Gerdhem P, Luthman H, Akesson K, Variation in the BMP2 gene: bone mineral density and ultrasound in young adult and elderly women., Calcif. Tissue Int. 81 (2007) 254–62. 10.1007/s00223-007-9054-9. [PubMed: 17726567]

[5]. Varanasi SS, Tuck SP, Mastana SS, Dennison E, Cooper C, Vila J, Francis RM, Datta HK, Lack of association of bone morphogenetic protein 2 gene haplotypes with bone mineral density, bone loss, or risk of fractures in men., J. Osteoporos. 2011 (2011) 243465. 10.4061/2011/243465. [PubMed: 22013543]

[6]. Xiong D-H, Shen H, Zhao L-J, Xiao P, Yang T-L, Guo Y, Wang W, Guo Y-F, Liu Y-J, Recker RR, Deng H-W, Robust and comprehensive analysis of 20 osteoporosis candidate genes by very high-density single-nucleotide polymorphism screen among 405 white nuclear families identified significant association and gene-gene interaction., J. Bone Miner. Res. 21 (2006) 1678–95. 10.1359/jbmr.060808. [PubMed: 17002564]

[7]. Mitchell BD, Streeten EA, Clinical impact of recent genetic discoveries in osteoporosis., Appl. Clin. Genet. 6 (2013) 75–85. 10.2147/TACG.S52047. [PubMed: 24133373]

[8]. Choi J-Y, Shin CS, Hong Y-C, Kang D, Single-Nucleotide Polymorphisms and Haplotypes of Bone Morphogenetic Protein Genes and Peripheral Bone Mineral Density in Young Korean Men and Women, Calcif. Tissue Int. 78 (2006) 203–211. 10.1007/s00223-005-0139-z. [PubMed: 16604289]

[9]. Ichikawa S, Johnson ML, Koller DL, Lai D, Xuei X, Edenberg HJ, Hui SL, Foroud TM, Peacock M, Econs MJ, Polymorphisms in the bone morphogenetic protein 2 (BMP2) gene do not affect bone mineral density in white men or women, Osteoporos. Int 17 (2006) 587–592. 10.1007/s00198-005-0018-5. [PubMed: 16432645]

[10]. Medici M, van Meurs JB, Rivadeneira F, Zhao H, Arp PP, Hofman A, Pols HA, Uitterlinden AG, BMP-2 gene polymorphisms and osteoporosis: the Rotterdam Study., J. Bone Miner. Res. 21 (2006) 845–54. 10.1359/jbmr.060306. [PubMed: 16753015]

[11]. Li GHY, Deng H-W, Kung AWC, Huang Q-Y, Identification of genes for bone mineral density variation by computational disease gene identification strategy., J. Bone Miner. Metab. 29 (2011) 709–16. 10.1007/s00774-011-0271-y. [PubMed: 21638018]

[12]. Bandyopadhyay A, Tsuji K, Cox K, Harfe BD, Rosen V, Tabin CJ, Genetic analysis of the roles of BMP2, BMP4, and BMP7 in limb patterning and skeletogenesis., PLoS Genet. 2 (2006) e216. 10.1371/journal.pgen.0020216. [PubMed: 17194222]

[13]. Tsuji K, Bandyopadhyay A, Harfe BD, Cox K, Kakar S, Gerstenfeld L, Einhorn T, Tabin CJ, Rosen V, BMP2 activity, although dispensable for bone formation, is required for the initiation of fracture healing., Nat. Genet. 38 (2006) 1424–9. 10.1038/ng1916. [PubMed: 17099713]

[14]. Feng J, Yang G, Yuan G, Gluhak-Heinrich J, Yang W, Wang L, Chen Z, Schulze McDaniel J, Donly KJ, Harris SE, Macdougall M, Chen S, Abnormalities in the enamel in bmp2-deficient mice., Cells. Tissues. Organs. 194 (2011) 216–21. 10.1159/000324644. [PubMed: 21597270]

[15]. Yang W, Guo D, Harris MA, Cui Y, Gluhak-Heinrich J, Wu J, Chen X-D, Skinner C, Nyman J, Edwards JR, Mundy GR, Lichtler A, Kream B, Rowe D, Kalajzic I, David V, Quarles D, Villareal D, Scott G, Ray M, Liu S, Martin JF, Mishina Y, Harris SE, Bmp2 gene in osteoblasts of periosteum and trabecular bone links bone formation to vascularization and mesenchymal stem cells., J. Cell Sci. (2013). 10.1242/jcs.118596.

[16]. McBride SH, McKenzie JA, Bedrick BS, Kuhlmann P, Pasteris JD, Rosen V, Silva MJ, Long Bone Structure and Strength Depend on BMP2 from Osteoblasts and Osteocytes, but Not Vascular Endothelial Cells, PLoS One. 9 (2014) e96862. 10.1371/journal.pone.0096862. [PubMed: 24837969]

[17]. Intini G, Nyman JS, Dkk1 haploinsufficiency requires expression of Bmp2 for bone anabolic activity, Bone. 75 (2015) 151–160. 10.1016/j.bone.2015.01.008. [PubMed: 25603465]

[18]. Salazar VS, Capelo LP, Cantù C, Zimmerli D, Gosalia N, Pregizer S, Cox K, Ohte S, Feigenson M, Gamer L, Nyman JS, Carey DJ, Economides A, Basler K, Rosen V, Reactivation of a developmental bmp2 signaling center is required for therapeutic control of the murine periosteal niche, Elife. 8 (2019). 10.7554/eLife.42386.

[19]. McBride-Gagyi SH, McKenzie JA, Buettmann EG, Gardner MJ, Silva MJ, Bmp2 conditional knockout in osteoblasts and endothelial cells does not impair bone formation after injury or mechanical loading in adult mice, Bone. 81 (2015) 533–543. 10.1016/j.bone.2015.09.003. [PubMed: 26344756]

[20]. McBride-Gagyi SH, Lynch ME, Biomechanical Principles of Fracture Healing, in: Crist BD, Borrelli J, Harvey E (Eds.), Essent. Biomech. Orthop. Trauma, 1st ed., Springer International Publishing, 2020: pp. 3–15. 10.1007/978-3-030-36990-3.

[21]. McCalden RW, McGlough JA, Barker MB, Court-Brown CM, Age-related changes in the tensile properties of cortical bone. The relative importance of changes in porosity, mineralization and microstructure, J. Bone Jt. Surg. - Ser. A. 75 (1993) 1193–1205. 10.2106/00004623-199308000-00009.

[22]. Schneider P, Voide R, Stampanoni M, Donahue LR, Müller R, The importance of the intracortical canal network for murine bone mechanics, Bone. 53 (2013) 120–128. 10.1016/j.bone.2012.11.024. [PubMed: 23219945]

[23]. Zhang X, Xie C, Lin ASP, Ito H, Awad H, Lieberman JR, Rubery PT, Schwarz EM, O'Keefe RJ, Guldberg RE, Periosteal progenitor cell fate in segmental cortical bone graft transplantations: implications for functional tissue engineering., J. Bone Miner. Res. 20 (2005) 2124–37. 10.1359/JBMR.050806. [PubMed: 16294266]

[24]. Ritchie RO, Koester KJ, Ionova S, Yao W, Lane NE, Ager JW, Measurement of the toughness of bone: a tutorial with special reference to small animal studies., Bone. 43 (2008) 798–812. 10.1016/j.bone.2008.04.027. [PubMed: 18647665]

[25]. Tang SY, Herber R-P, Ho SP, Alliston T, Matrix metalloproteinase-13 is required for osteocytic perilacunar remodeling and maintains bone fracture resistance., J. Bone Miner. Res. 27 (2012) 1936–50. 10.1002/jbmr.1646. [PubMed: 22549931]

[26]. McBride-Gagyi S, Toth Z, Kim D, Ip V, Evans E, Watson JT, Nicolaou D, Altering spacer material affects bone regeneration in the Masquelet technique in a rat femoral defect, J. Orthop. Res. 36 (2018) 2228–2238. 10.1002/jor.23866.

[27]. Berens P, CircStat : A MATLAB Toolbox for Circular Statistics , J. Stat. Softw. 31 (2009) 1–21. 10.18637/jss.v031.i10.

[28]. Ip V, Toth Z, Chibnall J, McBride-Gagyi S, Remnant woven bone and calcified cartilage in mouse bone: Differences between ages/sex and effects on bone strength, PLoS One. 11 (2016). 10.1371/journal.pone.0166476.

[29]. 000664 - C57BL/6J, (n.d.). https://www.jax.org/strain/000664 (accessed March 3, 2021).

[30]. Knippenberg M, Helder MN, Doulabi BZ, Bank RA, Wuisman PIJM, Klein-Nulend J, Differential Effects of Bone Morphogenetic Protein-2 and Transforming Growth Factor-β1 on Gene Expression of Collagen-Modifying Enzymes in Human Adipose Tissue–Derived Mesenchymal Stem Cells, Tissue Eng. Part A. 15 (2009) 2213–2225. 10.1089/ten.tea.2007.0184. [PubMed: 19231972]

[31]. Kaku M, Mochida Y, Atsawasuwan P, Parisuthiman D, Yamauchi M, Post-translational modifications of collagen upon BMP-induced osteoblast differentiation, Biochem. Biophys. Res. Commun. 359 (2007) 463–468. 10.1016/j.bbrc.2007.05.109. [PubMed: 17553463]

[32]. Jilka RL, O'Brien CA, Roberson PK, Bonewald LF, Weinstein RS, Manolagas SC, Dysapoptosis of Osteoblasts and Osteocytes Increases Cancellous Bone Formation But Exaggerates Cortical Porosity With Age, J. Bone Miner. Res. 29 (2014) 103–117. 10.1002/jbmr.2007. [PubMed: 23761243]

[33]. Salazar VS, Zarkadis N, Huang L, Norris J, Grimston SK, Mbalaviele G, Civitelli R, Embryonic ablation of osteoblast Smad4 interrupts matrix synthesis in response to canonical Wnt signaling and causes an osteogenesis-imperfecta-like phenotype., J. Cell Sci. 126 (2013) 4974–84. 10.1242/jcs.131953. [PubMed: 24006258]

[34]. Wang L, Mishina Y, Liu F, Osterix-Cre Transgene Causes Craniofacial Bone Development Defect, Calcif. Tissue Int. 96 (2015) 129–137. 10.1007/s00223-014-9945-5. [PubMed: 25550101] .

[35]. Huang W, Olsen BR, Skeletal defects in Osterix-Cre transgenic mice, Transgenic Res. 24 (2015) 167–172. 10.1007/s11248-014-9828-6. [PubMed: 25139670]

[36]. Davey RA, Clarke MV, Sastra S, Skinner JP, Chiang C, Anderson PH, Zajac JD, Decreased body weight in young Osterix-Cre transgenic mice results in delayed cortical bone expansion and accrual, Transgenic Res. 21 (2012) 885–893. 10.1007/s11248-011-9581-z. [PubMed: 22160436]

[37]. Wallace JM, Orr BG, Marini JC, Holl MMB, Nanoscale morphology of Type I collagen is altered in the Brtl mouse model of Osteogenesis Imperfecta., J. Struct. Biol. 173 (2011) 146–52. 10.1016/j.jsb.2010.08.003. [PubMed: 20696252]

[38]. Flurkey K, Currer JM, Harrison DE, Chapter 20 – Mouse Models in Aging Research, in: Fox JG, Davisson MT, Quimby FW, Barthold SW, Newcomer CE, Smith AL (Eds.), Mouse Biomed. Res, 2nd ed., Academic Press, Burlington, MA, 2007: pp. 637–672. 10.1016/B978-012369454-6/50074-1.

[39]. Klatte-Schulz F, Pauly S, Scheibel M, Greiner S, Gerhardt C, Hartwig J, Schmidmaier G, Wildemann B, Characteristics and Stimulation Potential with BMP-2 and BMP-7 of Tenocyte-Like Cells Isolated from the Rotator Cuff of Female Donors, PLoS One. 8 (2013). 10.1371/journal.pone.0067209.

[40]. Scibetta AC, Morris ER, Liebowitz AB, Gao X, Lu A, Philippon MJ, Huard J, Characterization of the chondrogenic and osteogenic potential of male and female human muscle-derived stem cells: Implication for stem cell therapy, J. Orthop. Res. 37 (2019) 1339–1349. 10.1002/jor.24231. [PubMed: 30667562]

Highlights

- BMP2 deficient bones are smaller and more brittle.
- Discrepancy in fracture toughness and size worsens for males from 10 to 15 weeks old but remains relatively stable for females between the two ages.
- BMP2 deficient bones are more porous with increased cellularity, more lacuna-scale voids, and more larger endosteal canals.

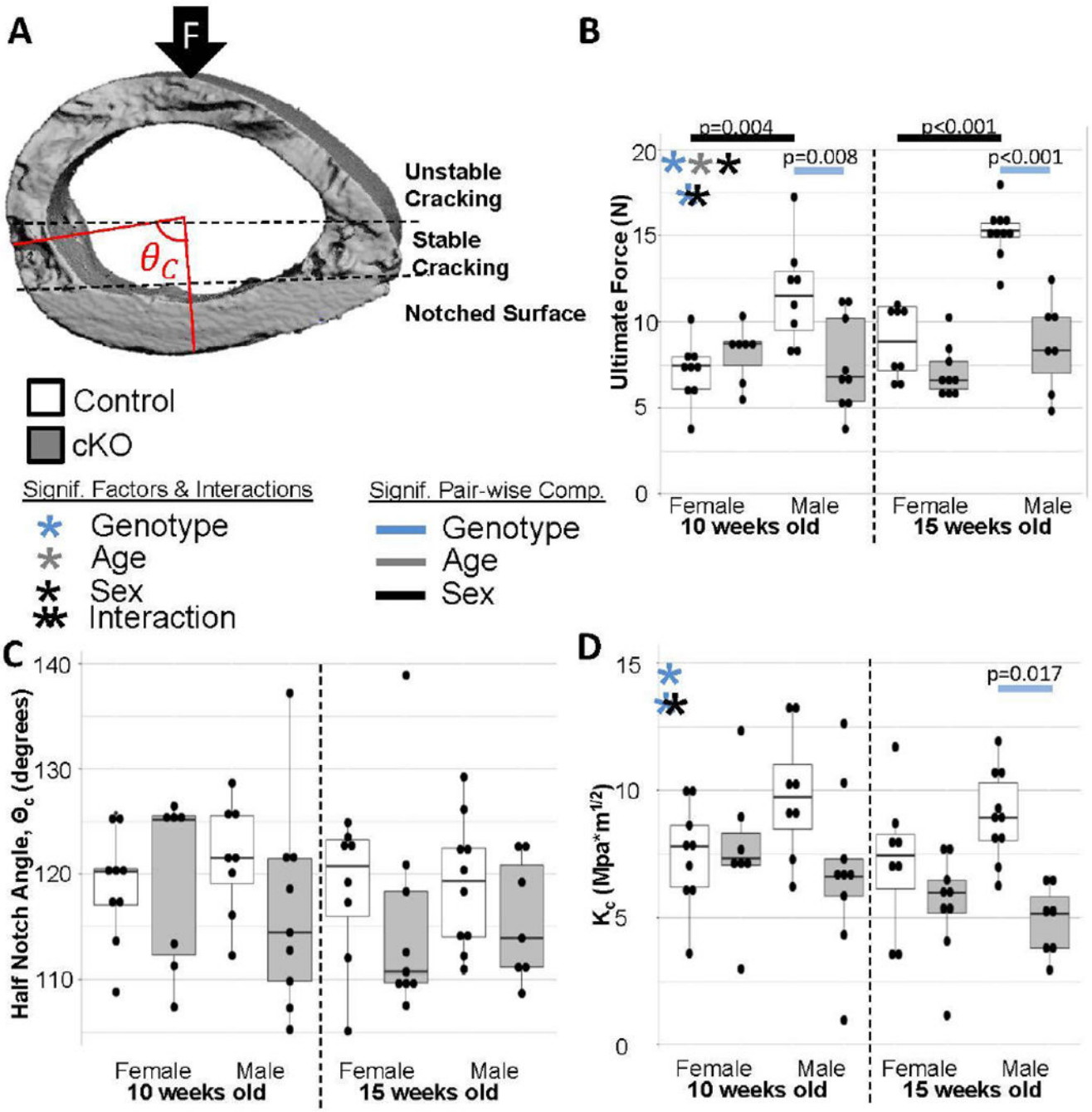

Figure 1. Fracture Toughness Testing.

(a) Example of 3D reconstruction used to measure half notch angle. The notched surface is the smooth surface on the bottom of the reconstruction. **(b)** In general cKO bones were weaker. **(c)** There were no differences in the half-notch angle. **(d)** Fracture toughness was generally lower in cKO bones confirming the previous findings that BMP2 knockout caused increased brittleness. Females maintained a similar differential between ages while the gap widened for males from 10 to 15 weeks.

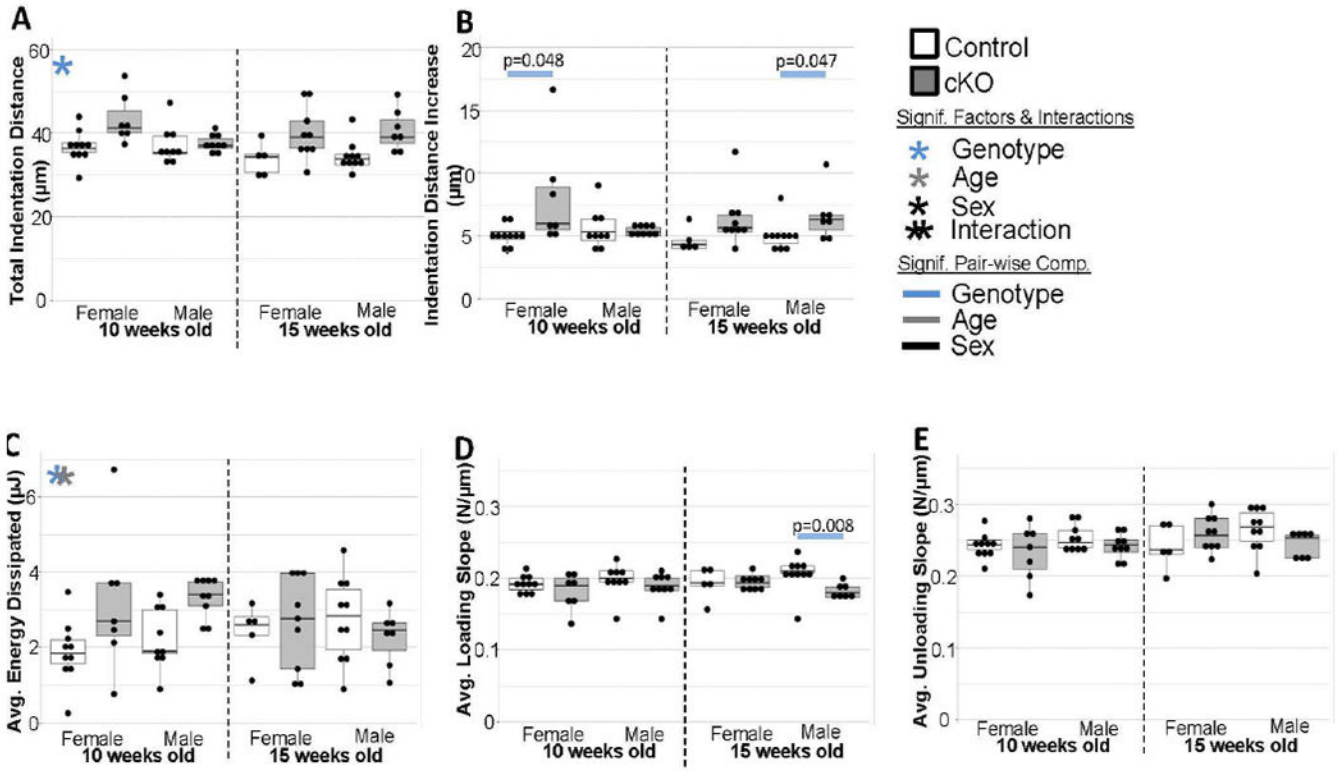

Figure 2. Reference Point Indentation.

(a) Total Indentation Distance was higher in cKO bones although the functional difference at the whole bone level is unclear. **(b)** Indentation distance increase was significantly increased in cKOs for the 10wk females and 15 wk males. There were few to no differences for average energy dissipated **(c),** average loading **(d),** or average unloading slope **(e)**.

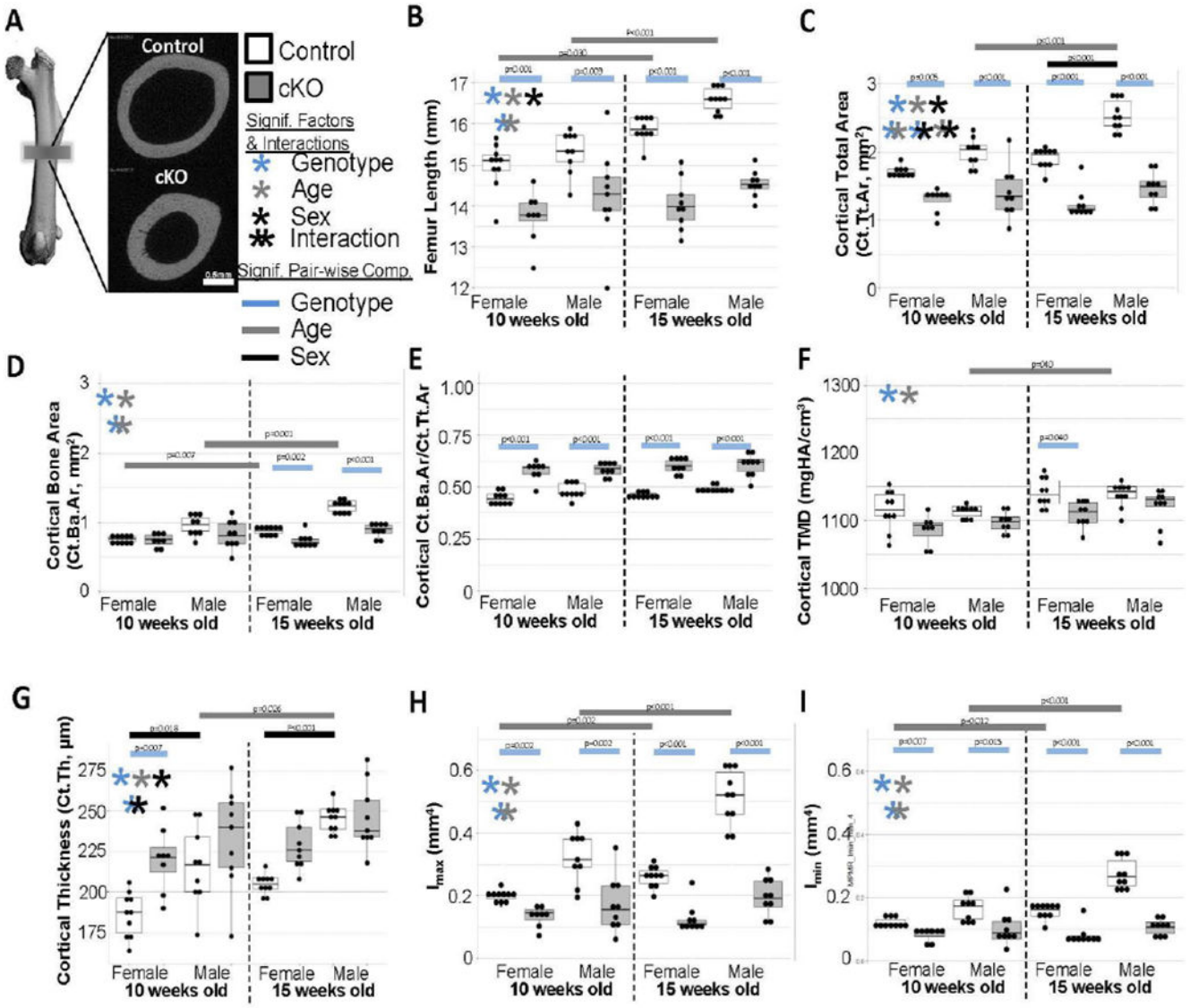

Figure 3. Medium Resolution MicroCT Results.

(a) Examples of midpoint morphology from control and cKO femora. **(b)** Femora were significantly shorter in cKO bones and did not lengthen as expected between the ages. **(c)** Similar deficits in total cross-sectional area and growth were observed. **(d)** Bone area had similar but less dramatic trends. **(e)** Ultimately, bone volume fraction was significantly increased for cKO in all groups. **(f)** Generally TMD was reduced in cKO bones. **(g)** As observed in panel A, cortical thickness was generally increased in cKO bones. **(h,i)** As expected with the smaller geometry, moments of inertia were reduced in cKO bones of all groups and did not increase with aging.

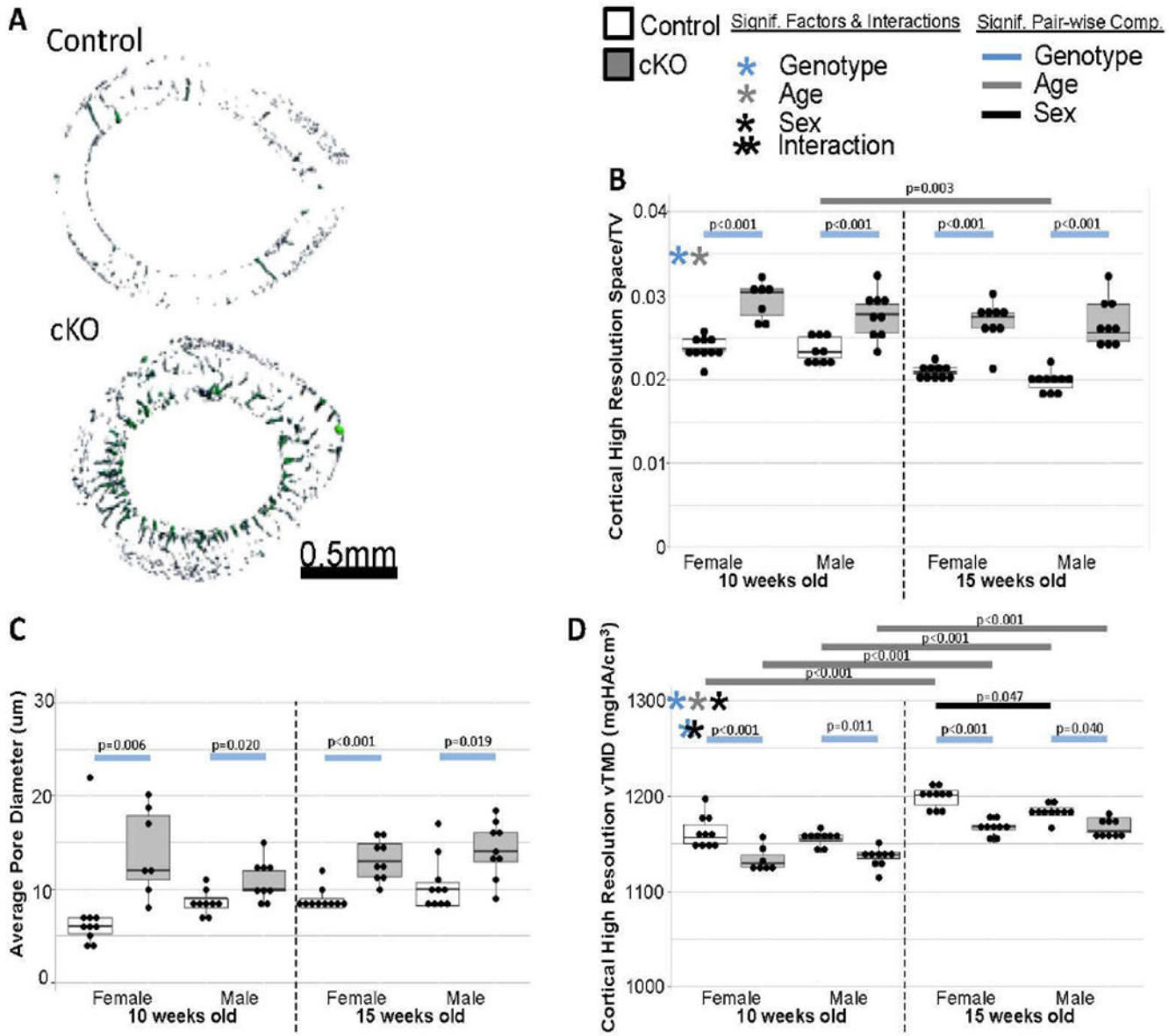

Figure 4. High Resolution MicroCT Results.

(a) Examples of midpoint space from control and cKO femora. **(b)** Femora from cKO bones had a significantly higher space volume fraction. **(c)** Average pore diameter was significantly increased in all cKO bones. **(d)** With the better capability of removing the small void partial volume effects, the lower TMD in cKO bones is more evident.

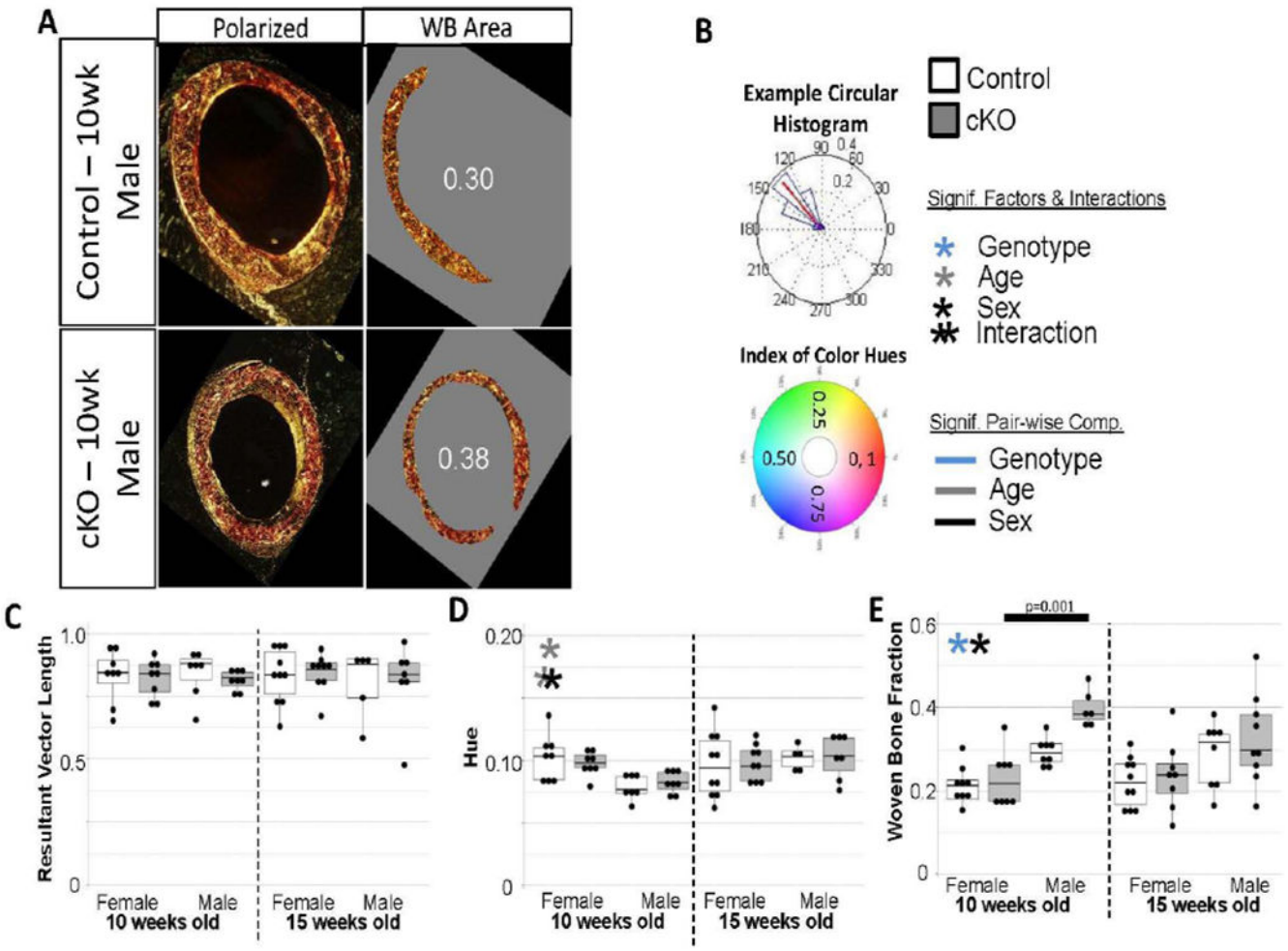

Figure 5. Polarized Light Imaging Results.

(a) Examples of polarized light images from control and cKO bones used to determine collagen alignment/packing and remnant woven bone fraction. **(b)** Example of collagen alignment data output. Resultant vector is shown in red. If all collagen fibers were perfectly aligned, the resultant vector length would be 1. The color wheel on the bottom panel shows values for all hues on a range from 0 to 1. Hue is an indirect measurement of collagen fiber size or packing. There were no difference between collagen alignment **(c)** or hue **(d)**. **(e)** Remnant woven bone fraction generally was higher in cKO bones, but again the difference may not indicate a strong functional correlation.

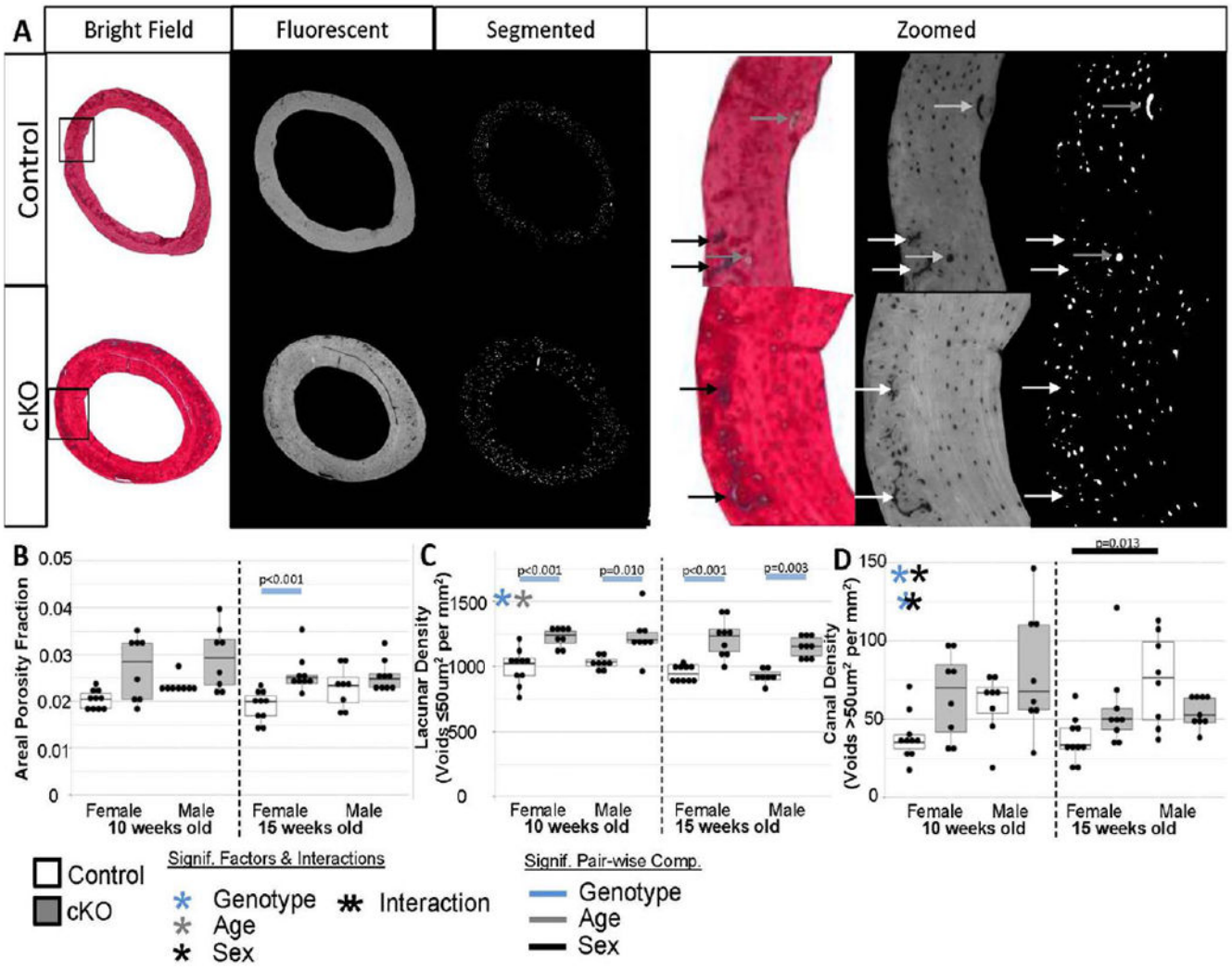

Figure 6. Fluorescent Light Imaging Results.

(a) Examples of sections imaged under fluorescent light to accentuate void areas. Calcified cartilage (black/white arrows), which is common in remnant woven bone bands, appeared as void spaces so were manually excluded from analysis. Larger canals (grey arrows) were included. **(b)** Overall areal porosity was not different between most groups. Although analysis as a whole was not possible due to the skewness of the data. This could also be a reflection of sectioning bias not capturing large canals well, which would constitute a large amount of the volumetric space. **(c)** Lacunae-scale void density was higher in all cKO bones which matched well the increase in cell nuclei. **(d)** Canal-scale void density was generally higher in cKO bones as observed in the high resolution microCT 3D reconstructions.

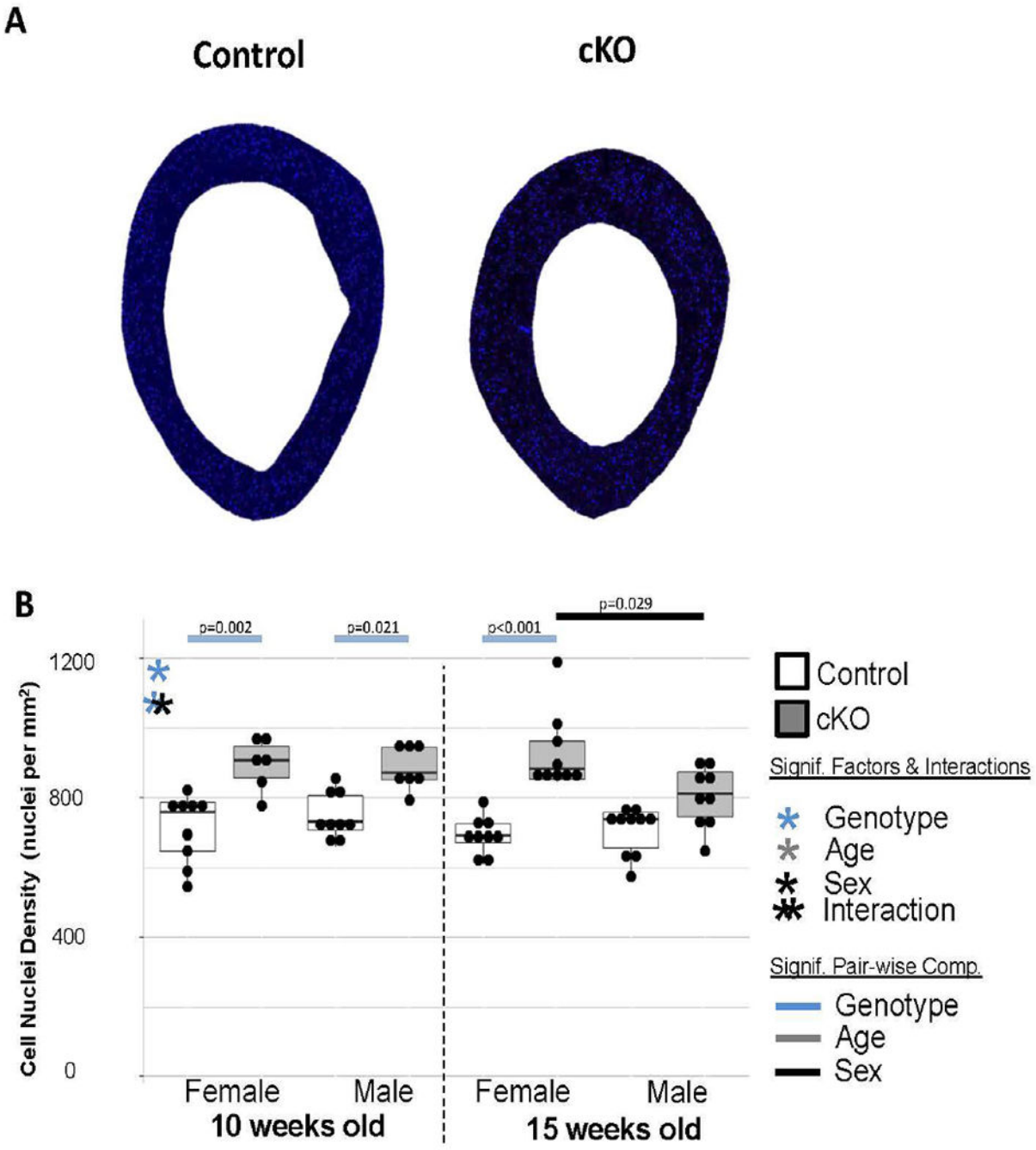

Figure 7. DAPI Section Results.

(a) Examples of DAPI sections imaged under fluorescent light to stain cell nuclei. **(b)** cKO bones consistently had more cells per unit area.

Table 1.

Details of Statistical Tests. Whenever possible the data was analyzed as a whole with no transformations with multi-variate ANOVA and post-hoc pair-wise comparisons. However, when the data did not meet assumptions of normality, first log-transformations were attempted. If that still did not meet normality, the data was continually split and transformed. If an outcome's data failed all other attempts to meet normality assumptions for ANOVA, the data for age/sex pairs were tested with Mann-Whitney. Bold p-values are significant.

Outcome	Statistical Test Used	Female/ Male Data	Was Data Log Transformed?	Factor & Interaction P-Values						
				Genotype	Age	Sex	Genotype:Age	Genotype:Sex	Age:Sex	Genotype:Age:Sex
Ultimate Force	ANOVA	Combined	Yes	**<0.001**	**0.012**	**<0.001**	0.062	**<0.001**	0.158	0.428
Half Notch Angle, Θ_c	ANOVA	Combined	No	0.129	0.343	0.861	0.798	0.440	0.927	0.484
K_c	ANOVA	Combined	No	<0.001	0.058	0.164	0.236	0.017	0.840	0.764
Total Indentation Distance	ANOVA	Combined	Yes	<0.001	0.194	0.355	0.203	0.202	0.156	0.196
Indentation Distance Increase	M-W		No							
Avg. Energy Dissipated	ANOVA	Combined	Yes	0.053	0.892	0.239	**0.024**	0.577	0.447	0.661
Avg. Loading Slope	M-W		No							
Avg. Unloading Slope	ANOVA	Combined	No	0.286	0.069	0.348	0.553	0.127	0.608	0.149
Femur Length	ANOVA	Combined	No	**<0.001**	**<0.001**	**<0.001**	**0.007**	0.939	0.502	0.483
Cortical Total	ANOVA	Combined	No	**<0.001**	**<0.001**	**<0.001**	**<0.001**	**0.007**	**0.024**	0.302
Area (MR MicroCT)										
Cortical Bone Area (MR MicroCT)	ANOVA	Female	No	**0.005**	**0.015**		**0.021**			
	ANOVA	Male	No	**<0.001**	**<0.001**		**0.033**			
Cortical Ba.Ar/Tt. Ar	M-W		No							
Cortical TMD (MR MicroCT)	ANOVA	Combined	No	**<0.001**	**<0.001**	0.398	0.835	0.170	0.948	9860.986
Cortical Thickness (MR MicroCT	ANOVA	Combined	No	**<0.001**	**<0.001**	**<0.001**	0.146	**0.023**	0.396	0.719
I_{max}	ANOVA	Female	No	**<0.001**	**0.010**		**0.004**			
	ANOVA	Male	No	**<0.001**	**<0.001**		**0.003**			
I_{min}	ANOVA	Female	No	**<0.001**	**0.035**		**0.019**			

Outcome	Statistical Test Used	Female/ Male Data	Was Data Log Transformed?	Factor & Interaction P-Values						
				Genotype	Age	Sex	Genotype:Age	Genotype:Sex	Age:Sex	Genotype:Age:Sex
	ANOVA	Male	Yes	**<0.001**	**<0.001**		**0.001**			
Cortical High Resolution Space/TV (HR MicroCT)	ANOVA	Combined	No	**<0.001**	**<0.001**	0.064	0.100	0.960	0.808	0.163
Average Pore Diameter (HR MicroCT	M-W		No							
Cortical High Resolution TMD	ANOVA	Combined	No	**<0.001**	**<0.001**	**0.033**	0.906	**0.017**	0.309	0.574
Resultant Vector Length	M-W		No							
Hue	ANOVA	Combined	No	0.881	**0.043**	0.093	0.622	0.617	**0.006**	0.578
Remnant Woven Bone Fraction	ANOVA	Combined	No	**0.021**	0.583	**<0.001**	0.426	0.152	0.200	0.338
Areal Porosity Fraction	M-W		No							
Lacunar Density	ANOVA	Combined	No	**<0.001**	**0.028**	0.598	0.549	0.423	0.210	0.834
Canal Density	ANOVA	Combined	Yes	**0.011**	0.550	**<0.001**	0.140	**0.020**	0.773	0.272
Cell Nuclei Density	ANOVA	Combined	No	**<0.001**	0.158	0.267	0.969	**0.013**	0.102	0.211